Mechanical spectroscopy observation of LiAlH$_4$ decomposition

Enrico Gianfranco Campari [a, *], Ennio Bonetti [a], Angelo Casagrande [b], Loris Ferrari [a], Giuseppe Levi [a]

[a] *Dipartimento di Fisica ed Astronomia, Bologna University, Viale Berti Pichat 6/2, Bologna, Italy*
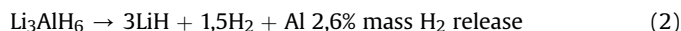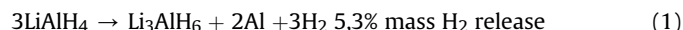[b] *Dipartimento di Ingegneria Industriale Viale Risorgimento 4, Bologna, Italy*

ABSTRACT

Dynamic elastic modulus and internal friction of cold consolidated mixtures of Al and LiAlH$_4$ powders have been measured. All reactions and decompositions occurring in LiAlH$_4$ during a thermal run have been detected as dynamic elastic modulus anomalies and internal friction peaks, proving the effectiveness of mechanical spectroscopy for the study of alanate. These informations are complementary to calorimetric and thermogravimetric data.

© 2019 Elsevier B.V. All rights reserved.

1. Introduction

Hydrogen is considered to be the fuel of the future. Its combustion with Oxygen is pollution free and the energy density is the highest among the elements: only 8,82 Kg of H$_2$ must be oxidized to yield a GJ of energy [1]. Yet the lack of an effective method for storing Hydrogen is restraining its employ for applications such as the automotive [2,3]. A widespread ongoing research is therefore devoted to find a way to store Hydrogen in solid state hydride materials. The successful material should have nearly ambient operating temperature, high reversibility storage capacity, fast kinetics, acceptable safety [4].

An interesting class of compounds are group I and II salts of [AlH4]$^-$, [NH2]$^-$, and [BH4]$^-$ (alanates, amides, and borohydrides, usually referred to as complex hydrides). They have recently received considerable attention as potential Hydrogen storage materials. In particular, LiAlH$_4$ has an overall H$_2$ mass release of more than 10% in three steps:

$$3LiAlH_4 \rightarrow Li_3AlH_6 + 2Al + 3H_2 \quad 5,3\% \text{ mass } H_2 \text{ release} \quad (1)$$

$$Li_3AlH_6 \rightarrow 3LiH + 1,5H_2 + Al \quad 2,6\% \text{ mass } H_2 \text{ release} \quad (2)$$

$$LiH + Al \rightarrow LiAl + (\tfrac{1}{2})H_2 \quad 2,6\% \text{ mass } H_2 \text{ release} \quad (3)$$

The three decompositions were observed by various research groups at slightly different temperatures. In the present work the first decomposition is observed at 440−450 K, the second at 480−490 K and the third at 645−670 K, in agreement with values reported into the literature [5−8]. Step (1) is a rather complex process where alanate melts and then decomposes. This decomposition is exothermic with a reported enthalpy variation of −10 kJ/mol, while reaction (2) is endothermic with an enthalpy variation of 25 kJ/mol [6]. These two reactions are those of interest for potential applications of alanate as a Hydrogen storage media. Step (3) is usually not considered as its temperature is too high for practical purposes.

Although LiAlH$_4$ is one of the most interesting candidate hydrides for solid state Hydrogen storage, its high capacity is plagued by drawbacks such as exothermic reactions, relatively slow Hydrogen desorption rate and irreversibility of the decomposition in practical conditions. Several routes have been attempted in order to overcome these limitations, including doping with several additives such as TiO, BN, Fe oxides or the use of milled alanate nanoparticles [6,8−10]. At the same time, many efforts are being performed in order to better understand the system evolution, which is highly dependent on parameters such as impurities,

---

* Corresponding author. Physics and Astronomy Department, Bologna University, Viale Berti Pichat 6/2, I-40127, Bologna, Italy.
E-mail address: enrico.campari@unibo.it (E.G. Campari).

heating rates, pressure, powder morphology [6,8,9,11].

Beside its use as an energy carrier, LiAlH$_4$ is widely used as a strong reducing agent in organic synthesis for the reduction of esters, carboxylic acids, and amides [12,13]. It will reduce almost any C=O containing functional group to an alcohol.

A complementary technique for the characterization of materials properties, mechanical spectroscopy investigation can be performed together and in parallel with calorimetric measurements. Mechanical spectroscopy is a tool able to effectively probe many properties of materials, since the elastic constants and the damping of vibrations are sensitive to measurable quantities such as the atomic arrangement, composition or magnetic coupling. By mechanical spectroscopy we refer to the measure of the internal dissipation of the vibrational energy of a given specimen, usually as a function of temperature or frequency. From the resonance frequency, density and shape of the specimen, the dynamic elastic modulus of a material is obtained, together with the damping or internal friction. The technique is really sensitive and can usually provide more precise data than those obtained with DSC (differential scanning calorimetry) and TGA (thermogravimetric analysis). Some previous and closely related work on LiAlH$_4$ and NaAlH$_4$ was performed indeed with this technique in recent years [14]. It demonstrated how mechanical spectroscopy is effective to study the Hydrogen dynamics and the onset of the decomposition reactions.

A phase transformation in a solid is usually coupled to a damping peak and to a sharp variation or discontinuity in the modulus [15,16]. More specifically, a first order transformation, like melting, is accompanied at the transition temperature by a damping peak and a jump in the dynamic elastic modulus, while a higher order transformation such as a crystal symmetry change exhibits a downward lambda shaped modulus curve together with a damping peak or upward divergence [17,18]. An order-disorder transformation may display a discontinuity in both quantities [19].

Amongst first order transitions, the study of melting requires the use of some shrewdness. The matter of measuring a specimen which undergoes melting has been handled in several ways. One is to cast the substance to be measured inside a hollow reed of stainless steel closed to an end [18]. A different strategy consists in mixing and melting two materials with different melting temperatures in order to obtain, after cooling, a specimen with two phases to be subsequently measured [20,21]. Unfortunately, none of these procedures is appropriate for the case of alanate for two reasons. First of all, the material releases a great amount of Hydrogen and then, in ordinary conditions, its decompositions are irreversible. We therefore proceed by mixing Aluminum and LiAlH$_4$ powders, with formation, after cold consolidation under a uniaxial pressure of about 1 GPa, of a composite structure made by an Aluminum matrix with interspersed alanate regions. The Aluminum matrix behaves as a backbone which provides the required mechanical strength which allows to measure alanate even through step (1) decomposition, which can be preceded by melting. In these conditions, experimental data contain the contribution of both materials and their decoupling is obtained from a measure of the container or the un-melting material alone.

The Purpose of this work is to study the various LiAlH$_4$ decompositions by means of mechanical spectroscopy measurements. It will be shown how this technique is able to provide both complementary and useful data with respect to those usually achieved with calorimetric techniques. The measurement of elastic constants and their variations in order to explain and quantify the development of chemical-physical phenomena as a function of the temperature, not only provides new and additional informations, but also helps to immediately visualize the development of chemical-physical events while providing very precise analytical measurements of the same events. As is known, conventional thermal techniques are particularly sensitive to minimal variations in the choice of test parameters and often the expected events cannot be properly documented.

2. Experimental

As received commercial Alfa Aesar LiAlH$_4$ powders (97% purity) are used, without any further purification, for all measurements presented in this work. Powders and specimens are kept and handled under a vacuum or in a dry box in order to avoid reaction with moisture. For all mechanical tests, specimens are prepared mixing from 40 to 60 mg of LiAlH$_4$ with 200−350 mg Al (purity >99,9% weight) and then cold consolidated under a uniaxial pressure of about 1 Gpa. The compacted reeds dimensions are: $30,0 \times 6,0$ mm^2 surface area and 0,7 to 1,0 mm thickness. Due to the lower density of alanate with respect to that of Aluminum (roughly one third), the starting volumes of the mixed compounds are nearly the same. Specimens are not fully densified and, as a result, the dynamic elastic modulus of the specimens is rather low with respect to that of pure polycrystalline Aluminum specimens obtained from the melt, whose values range from 65 to 70 GPa. Typical values measured in the present work are in the range between 8 and 12 GPa with a relative uncertainty of 15%, with differences between specimens due to the different ratio between Aluminum and alanate and the applied pressure. These values are close to those reported for LiAlH$_4$ modulus, which is of the order of 12 GPa [22]. Much lower values of the Young's modulus with respect to those of solid materials obtained from the melt are, moreover, commonly reported for cold consolidated powders, especially for the case of mixtures without strong chemical bonds between different phases [23,24].

Mechanical measurements are performed in a vacuum by means of the mechanical analyzer VRA 1604 [25,26] or in Argon/dry air by means of DMA (Dynamic Mechanical Analyzers) Q800 by TA Instruments [27]. The internal friction (usually referred to as IF or Q^{-1}) is defined as Q^{-1} = (ΔW/2πW) where W is the elastic energy stored in a specimen and ΔW is its decrease during an oscillation. It can be obtained in a resonant experiment, as is the case for VRA, from the envelope of the decreasing oscillation amplitude of the specimen when excitation is turned off. Its value is given by (d/π)i, where d = ln (A$_n$/A$_{n+1}$) is the logarithmic decrement of the oscillation amplitude, A$_n$, between the n-th and (n+1)-th oscillation. In subresonant experiments (DMA), internal friction is obtained from the lag between the imposed stress σ = σ$_0$ e$^{i\omega t}$ and the resulting strain ε = ε$_0$ e$^{i(\omega t - \phi)}$. When the damping is much smaller than one, Q^{-1} = tanϕ ≅ ϕ and the values computed by the two methods are equal [14,28].

In the VRA apparatus, specimens are mounted in free-clamped mode and excited by flexural vibrations. Specimens are kept into resonance while temperature is changing at the selected rate. The resonance frequency of all specimens is in the 300−1500 Hz range; the strain amplitude is about 10^{-5}. Samples are heated from room temperature up to a maximum temperature of 750 K at 2 K/min rate.

In the DMA apparatus, specimens are mounted in single cantilever bending and excited in forced vibration mode at 10 Hz frequency. The applied strain amplitude is higher with respect to that used for VRA, mainly because of the need to obtain a better signal to background ratio, taking care of air damping. Values of about $2 \cdot 10^{-4}$ are used in most cases. Despite the Aluminum internal friction strain dependence, the alanate contribution to the signal remains unchanged both at the high and the low strain values. Specimens are heated from room temperature up to 600 K at a constant rate of 2 or 3 K/min, Fig. 1a and b shows two specimens as

(a) **(b)**
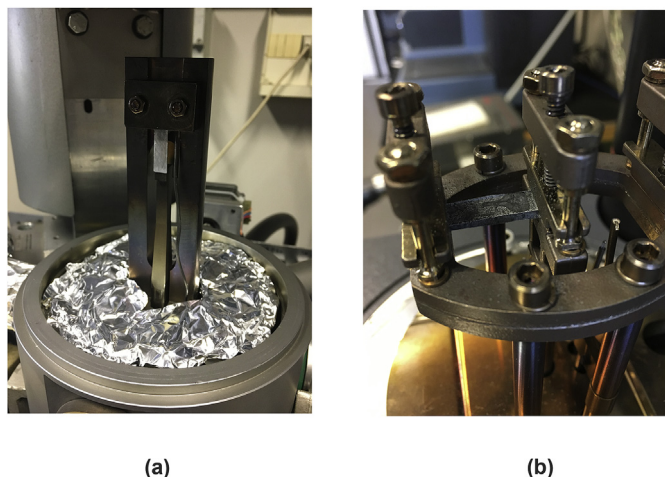
Fig. 1. Images of cold consolidated specimens made starting from Al + LiAlH$_4$ powders. In (a) specimen is vertically mounted in free cantilever mode inside the VRA apparatus, while in (b) it is orizontally mounted in single cantilever mode inside the DMA apparatus. Both pictures were taken at the end of a thermal run up to 700 K. Clearly visible on the surface of the latter specimen are the signs of fusion and Hydrogen release.

they appear at the end of a thermal run in the VRA and DMA mounting, respectively.

DSC (differential scanning calorimetry) and TGA (thermogravimetric analysis) reference tests on Al and LiAlH$_4$ are performed with both an SDT Q600 and a Q10 instrument by TA Instruments in flowing Argon atmosphere [29]. Sample mass is typically 5−6 mg and heating rate from 2 to 5 K/min.

Alanate and compacted Al + LiAlH$_4$ powders morphology are examined by scanning electronic microscopy (SEM) with a ZAISS EVO 50 apparatus operating at 20 kV equipped with an EDS (energy dispersive spectrometer) INCA X-ACT from OXFORD INSTRUMENTS.

3. Results and discussion

3.1. Morphology and microstructure of LiAlH$_4$ and Al + LiAlH$_4$ mixtures

Fig. 2 shows an electron microscope image of the as received
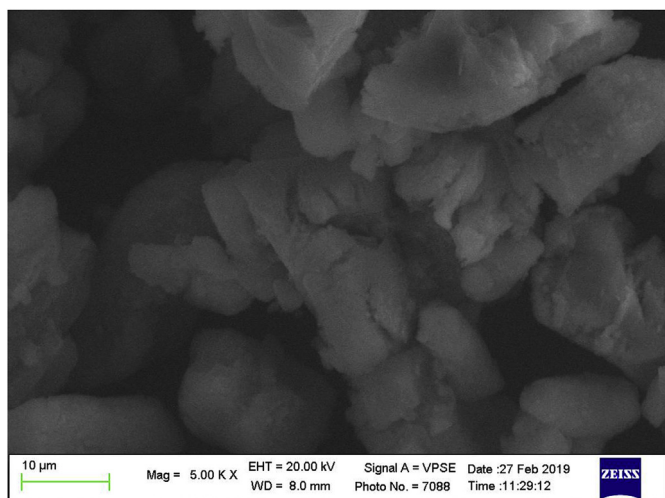
powders. Grains of a few micrometers are visible, with the same morphology usually observed for commercial powders, resulting from the monoclinic crystal lattice of LiAlH$_4$ [8,30]. Fig. 3 shows a two phases specimen as obtained after mixing alanate powders with Aluminum powders and successive cold consolidation. An Aluminum matrix (brighter areas) is observed with interspersed darker regions of alanate.

After thermally treating the alanate powders and the compressed specimens up to 580 K, a rather different morphology is obtained. The high exothermicity of the lowest temperature decomposition reaction has significantly modified the morphology of LiAlH$_4$ powders, as can be seen in Fig. 4, making them referable to softening and melting phenomena. The images of the morphologically modified powders highlight spherical formations and a much finer dimension than the starting ones with the ability to weld, as if a fast melting phenomenon was produced. Signs of fusion are also present in the compressed mixtures, as can be seen in Fig. 1b, relative of a specimen measured with DMA in dry air. At a microscopic level, thermally treated cold consolidated specimens exhibits a diffuse presence of cracks or pore-like features which ought to be due to Hydrogen outflow from the specimen inside, see Fig. 5.

3.2. Mechanical tests and calorimetry

The LiAlH$_4$ decomposition with Hydrogen release of steps (1) to (3) has been extensively studied in recent years by means of DSC and TGA apparatuses. Step (1), occurring at the lowest temperature, is both the most interesting and complex. In a typical heating test at 5−10 K/min heating rate, an endothermic peak is commonly observed and attributed to melting of LiAlH$_4$. It is immediately followed, 5−15° higher in temperature, by an exothermic peak, due to its decomposition. A corresponding TGA measure shows in this temperature range a weight decrease due to Hydrogen desorption. In some cases, immediately before melting, an exothermic peak, attributed to the interaction of LiAlH$_4$ with surface hydroxyl impurities, is detected [8,10]. However, step (1) can occur differently at lower heating rates or in the presence of doping additions, of impurities or as a consequence of milling [8,11,30,32,33]. Hence, it is reasonable to assume that the decomposition can follow alternative routes, including ones that do not require the melting of LiAlH$_4$.

Fig. 2. SEM observation of as-received LiAlH$_4$ powders.
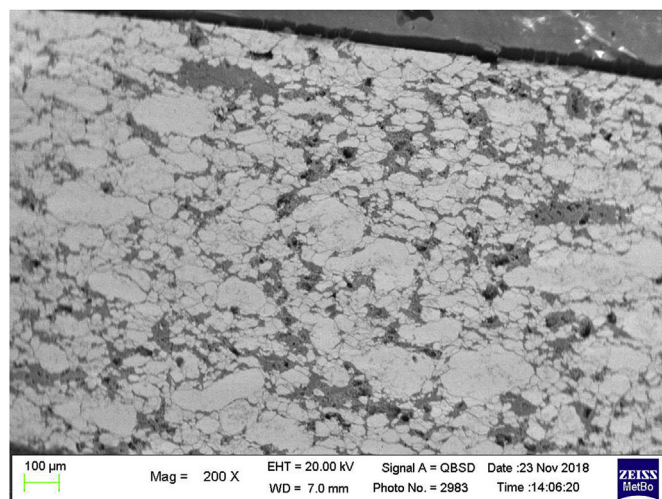
Fig. 3. Metallographic section, prepared by abrasion with emery papers with decreasing grain size and polishing by cloths with ceramic abrasive of the Al + LiAlH$_4$ composite after pressing at 1 Gpa. The brighter regions are Aluminum, the darker alanate.
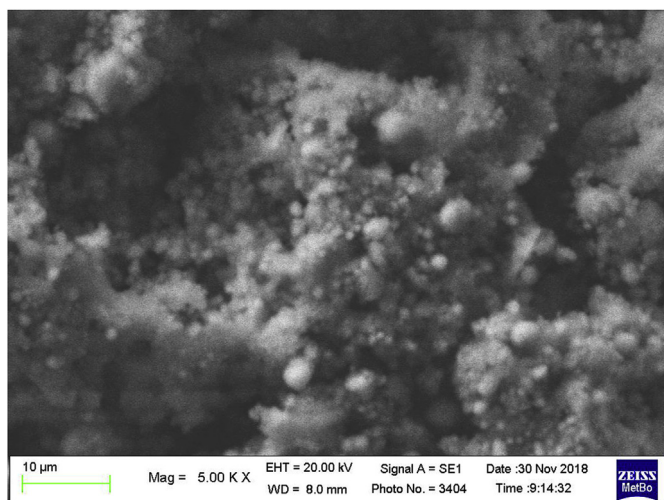
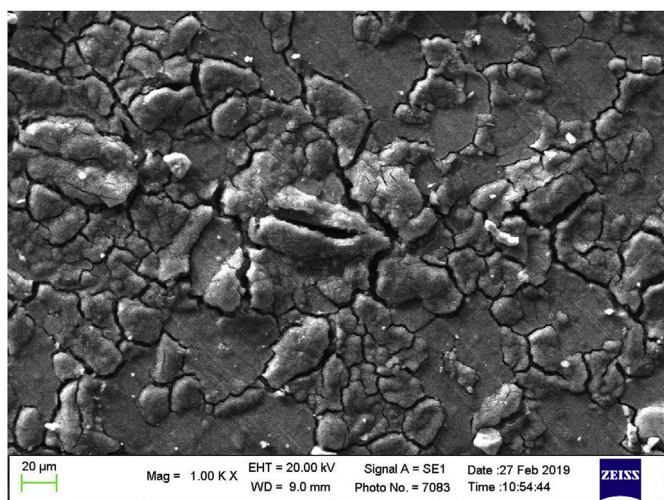**Fig. 4.** SEM observation of LiAlH$_4$ powders after a thermal heating up to 580 K.

Fig. 5. SEM observation of the surface of a cold consolidated Al + LiAlH$_4$ specimen, which exhibits a diffuse presence of cracks or pore-like features, due to Hydrogen outflow during stages (1) and (2). The specimen is heated in dry air inside the DMA apparatus at a heating rate of 3 K/min from room temperature up to 580 K. SEM observation is performed after cooling the specimen in dry air.

Reference DSC measures performed on the as-received alanate powders used for this work, show the usual decomposition process while in cold consolidated Al + LiAlH$_4$ mixtures, the endothermic peak immediately before LiAlH$_4$ decomposition is missing, see Fig. 6. The peak (here a shoulder at the left of the decomposition peak) usually assigned to the interaction of LiAlH$_4$ with surface hydroxyl impurities is also detected, together with the endothermic peak of step (2). The occurrence of Hydrogen release is confirmed by specimen mass decrease. DSC tests are performed in this work at rates of 2 or 3 K/min for comparison with mechanical tests, where higher rates are not commonly used in order to keep specimens at uniform temperature.

X ray diffraction (XRD) studies reported into literature of alanate specimens from room temperature up to 600 K, clearly show the disappearing of the LiAlH$_4$ phase followed by the appearing of the Li$_3$AlH$_6$ phase, which in turn disappears at higher temperatures to leave place to LiH [5,31,33]. A similar behavior is observed in other alanates [33,34]. As mentioned before, this standard transformation sequence can be deeply modified by changing powders
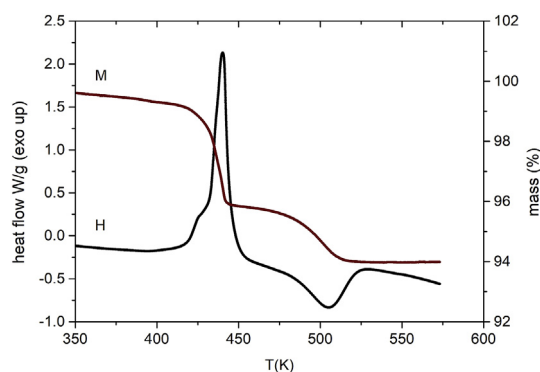

Fig. 6. DSC (H) and TGA (M) signals of a 6 mg specimen taken from a cold consolidated Al + LiAlH4 mixture. Heating rate 3 k/min. Aluminum pan.

morphology (e.g. by milling) or by dopant addition [6–10].

Figs. 7 and 8 show the corresponding mechanical behavior of an Al + LiAlH$_4$ specimen prepared by cold consolidation as described in the experimental section. Fig. 7 refers to a specimen measured under a vacuum in the VRA apparatus while Fig. 8 refers to a specimen measured in the DMA apparatus in dry air. Even if VRA reveals to be more sensitive, step (1) decomposition is clearly observed with both apparatuses. The following features are always present in a VRA measure:

1) a small damping peak with a corresponding modulus defect at about 380 K;
2) a damping maximum with a corresponding modulus steep decrease at about 430 K;
3) a damping upward spike with a corresponding downward modulus spike at about 445 K;
4) a second small damping peak with a corresponding modulus defect at about 480 K.

Twelve specimens with slightly different Al to LiAlH$_4$ ratios are measured with both apparatuses (six with VRA and six with DMA). The same features, with temperature differences in a range not greater than 10 K between measures, are found for all specimens. In the case of VRA measures, pressure values inside the vacuum chamber are also collected. A pressure peak is detected,
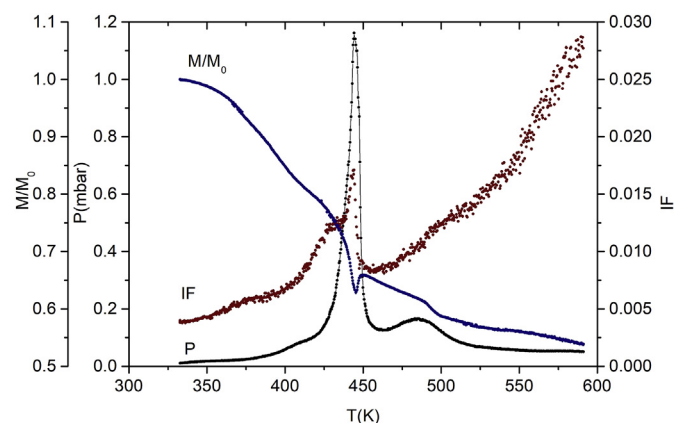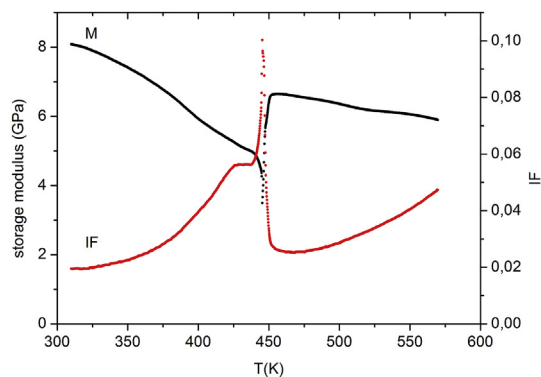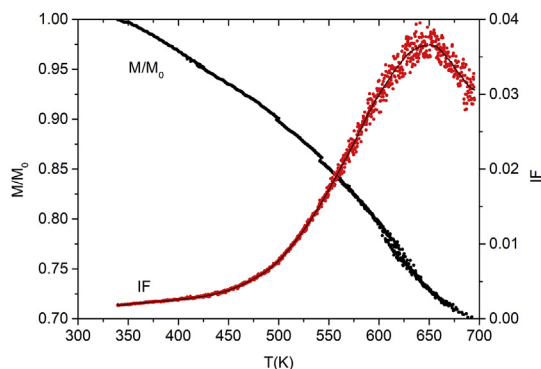

Fig. 7. Cold consolidated Al + LiAlH$_4$ powders specimen measured with the VRA apparatus in a vacuum at a heating rate of 1,5 k/min. The reported signals are: dynamic elastic modulus (M/M$_0$, blue dots) normalized to its starting value at room temperature; internal friction (IF, red dots); pressure (P, black dots). (For interpretation of the references to colour in this figure legend, the reader is referred to the Web version of this article.)
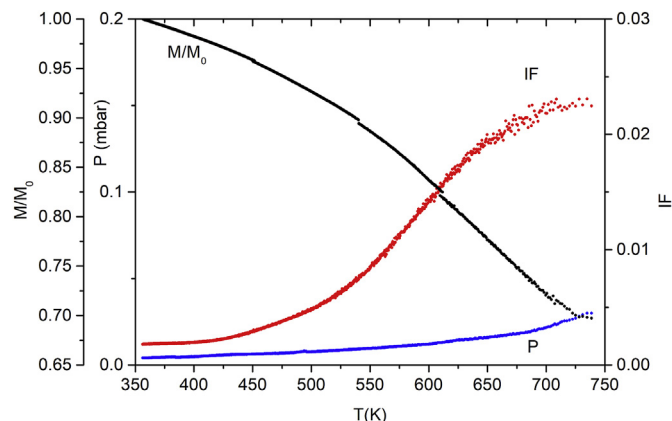
Fig. 8. Dynamic elastic modulus (M, black dots) and internal friction (IF, red dots) of a cold consolidated Al + LiAlH$_4$ powders specimen measured with the DMA apparatus in dry air. The dynamic modulus at room temperature is 8,1 GPa. Internal friction values are higher than those reported into Fig. 7 mainly because of a higher strain and air contribution. (For interpretation of the references to colour in this figure legend, the reader is referred to the Web version of this article.)

corresponding to each decomposition. The reported peaks are the fingerprints of Hydrogen desorption from LiAlH$_4$ and provide a valuable information about Hydrogen release. Peak height is proportional to the amount and rate of Hydrogen release.

Figs. 9 and 10 shows, for comparison, the mechanical behavior of pure cold consolidated Aluminum powders and that of a second thermal run up to about 750 K on an Al + LiAlH$_4$ mixture, respectively. The damping of pure Aluminum is well known from the literature and is characterized by an increasing background attributed to the bowing of dislocations and by a Debye peak generally attributed to grain boundary relaxation [15 ch. 15, 28 ch. 2, 35,36,37]. The dynamic modulus, normalized at its value at the beginning of each reported run, monotonously decreases as a function of temperature, as usually observed in solids. The decrease is steeper at the peak position (modulus defect). A similar behavior is measured on Al + LiAlH$_4$ mixtures after a first thermal run up to 750 K. This heat treatment induces a complete decomposition of alanate so that the specimen becomes a mixture of Aluminum and Lithium. Now, the damping grain boundary peak is broadened and shifted at higher temperatures. The dynamic modulus decreases with respect to that at the beginning of the first run, probably due to the pores and cracks produced by Hydrogen outflow, since Aluminum powders alone exhibits the expected increase. Both grain boundary peak and background are frequency dependent, as

Fig. 10. Second run data of a cold consolidated Al + LiAlH$_4$ powders specimen measured with the VRA apparatus in a vacuum at a heating rate of 1,5 K/min after a first heating in a vacuum at 1,5 K/min from room temperature up to 750 K. The reported signals are: dynamic elastic modulus (M/M$_0$, black dots) normalized to its starting value at room temperature; internal friction (IF, red dots); pressure (P, blue dots). (For interpretation of the references to colour in this figure legend, the reader is referred to the Web version of this article.)

observed in our measures and as reported into literature for thermally activated processes [15,28,38]. Specifically, the grain boundary peak in pure Aluminum has an activation energy of about 1,3−1,5 eV (125−145 kJ/mol), depending on Aluminum purity and specimen microstructure. At the opposite, features 2) to 4) do not depend on temperature, as can be evinced from the absence of any temperature shift for these features in DMA measures performed at 10 Hz and VRA measures performed at resonance frequencies up to 1500 Hz. Therefore, the data shown into Figs. 9 and 10 prove how features 2) to 4) are not due to Aluminum but reflect the LiAlH$_4$ thermal behavior.

Feature 1) is due to the relaxation of defects introduced by the cold consolidation process in Al cold consolidated powders. It is typical of Aluminum specimens and disappears after a heat treatment at or above 700 K [38].

After a first run up to 580 K, one of the specimens is thermally heated up to about 750 K in the VRA apparatus. Fig. 11 reports about this test. The LiH decomposition is revealed by both a pressure

Fig. 9. Dynamic elastic modulus (M/M$_0$, black dots) and internal friction (IF, red dots) reference data of a cold consolidated Al powders specimen measured with the VRA apparatus in a vacuum at a heating rate of 1,5 K/min. (For interpretation of the references to colour in this figure legend, the reader is referred to the Web version of this article.)
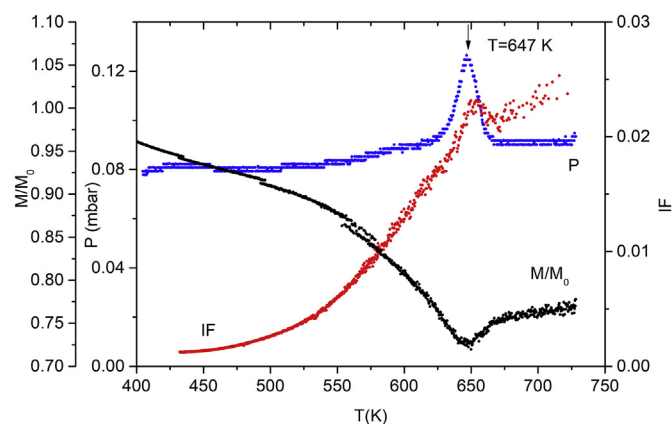

Fig. 11. Cold consolidated Al + LiAlH$_4$ powders specimen measured with the VRA apparatus in a vacuum at a heating rate of 1,5 K/min after a first heating in a vacuum at 1,5 K/min from room temperature up to 580 K. The reported signals are: dynamic elastic modulus (M/M$_0$, black dots) normalized to its starting value at room temperature; internal friction (IF, red dots); pressure (P, blue dots). Second run after a first heating up to 580 K. (For interpretation of the references to colour in this figure legend, the reader is referred to the Web version of this article.)

peak, a modulus softening and a damping increase at 647 K.

3.3. Damping and modulus behavior

A phase transition can usually be described by the use of one (and sometimes more than one) internal variable. In the case of a first order transition the internal variable undergoes a discontinuous change, while in a higher order transformation it remains continuous, even if its rate of change diverges. As far as internal variables, such as an order parameter, are coupled to the elastic constants of a material, large effects on modulus and damping are expected at the transition [14,39,40]. If the first order phase transition is a melting, elastic modulus exhibits a downward jump at the transition temperature, due to bonding breaking between atoms or molecules. This has been observed for metals such as Tin, Bismuth, Antimony, Lead, Indium and several eutectic alloys [18,41].

Alanate decomposition, step (1), exhibits some similarity with a so called "lambda point", typical of second order phase transitions, i.e. a cuspid singularity, upward directed for internal friction and downward directed for dynamic elastic modulus. According to phase-transition theories however, such singularities should be due to a bi-linear coupling between the stress field and the order parameter and should refer to reversible transitions. This is certainly not the case of the present transformation, which is manifestly irreversible, as shown by Figs. 7 and 10. So, the origin of the pseudo-lambda shape of the transformation (a softening, followed by a steep hardening of the structure, in a small temperature interval) is to be ascribed to the decomposition process, not involving a true phase transition. It is reasonable to relate such process to the breaking of the Hydrogen tetrahedrons about the Aluminum atoms (softening), and to the simultaneous formation of the new Li_3AlH_6 phase (hardening), which should result in the spherical aggregates morphology of the residual Alanate powders, as shown by Fig. 4. The nucleation and growth of a new phase is an example indeed of a process giving rise to internal friction effects.

As regard the specific mechanism causing the sudden damping increase, the presence of free Hydrogen must be taken into consideration. A number of different Hydrogen relaxation effects due to the motion of Hydrogen atoms in solids is known, from Snoek to Zener type relaxation to other coupled processes where Hydrogen atoms interact with dislocations or grain boundaries [28]. The sudden Hydrogen presence in the specimens due to the various decompositions could add a transient new term to the damping.

Cracks and pores generation due to Hydrogen outflow cannot be held responsible for the observed IF and dynamic elastic modulus features. A change in specimen connectivity would produce an irreversible modulus change, while we observe transient phenomena corresponding in time and temperature to the decomposition steps.

In summary, mechanical spectroscopy tests show that:

1. As suggested by an exact correspondence with the DSC feature usually attributed to the interaction of $LiAlH_4$ with surface hydroxyl impurities, feature 2) is the sign of that reaction as observed by mechanical spectroscopy.
2. Feature 3) corresponds to $LiAlH_4$ decomposition with Hydrogen release (pressure peak as detected in VRA tests). Two out of three of the Aluminum atoms get free from the Hydrogen tetrahedral cage (the AlH_4^- anions, where the Hydrogen atoms are tetrahedrally coordinated around the Al atom) [3], whose destruction causes the emission of Hydrogen and the measured pressure increase observed in Figs. 7 and 8. The irreversible

nature of the process, which is also frequency independent, is manifest.
3. Feature 4) corresponds to Li_3AlH_6 decomposition, with a new Hydrogen release. This is both proved from the pressure peak, see Fig. 7, and from the temperature coincidence with DSC and TGA measures.
4. At higher temperatures, see Fig. 11, the final decomposition of fcc LiH into Li and Hydrogen is detected. Even if less intense, these two last transformations closely resemble that of step (1), with a dynamic elastic modulus dip, a damping narrow peak and a pressure peak.

4. Conclusions

The decompositions occurring in $LiAlH_4$ as a function of temperature during heating has been directly measured for the first time by means of mechanical spectroscopy, performing tests on cold consolidated Aluminum and alanate powders having a composite morphology and a good mechanical strength. Mechanical spectroscopy data prove to be equally or more precise than calorimetric data and could help to characterize transformations whose details are not yet completely understood.

References

[1] http://www.eagle.ca/~gcowan/boron_blast.html.
[2] E.G. Campari, M. Bianchi, L. Tomesani, Energy Procedia 126 (2017) 541–548, https://doi.org/10.1016/j.egypro.2017.08.276.
[3] Jeung Ku Kang, Jai Young Lee, R.P. Muller, W.A. Goddard III, J. Chem. Phys. 121 (2004) 10623, https://doi.org/10.1063/1.1795731.
[4] Shin-ichi Orimo, Y. Nakamori, J.R. Eliseo, A. Zuttel, Craig M. Jensen, Chem. Rev. 107 (2007) 4111–4132, https://doi.org/10.1021/cr0501846.
[5] Hao Yao, S. Isobe, Y. Wang, N. Hashimoto, S. Ohnuki, Int. J. Hydrogen Energy 38 (2013) 3689–3694, https://doi.org/10.1016/j.ijhydene.2013.01.074.
[6] Y. Nakagawa, S. Isobe, T. Ohki, N. Hashimoto, Inorga 5 (2017) 71, https://doi.org/10.3390/inorganics5040071.
[7] Lei Wang, Kondo-Francois Aguey-Zinsou, Inorga 5 (2017) 38, https://doi.org/10.3390/inorganics5020038.
[8] Rafi-ud-din, Lin Zhang, Ping Li, Xuanhui Qu, J. Alloy. Comp. 508 (2010) 119–128, https://doi.org/10.1016/j.jallcom.2010.08.008.
[9] H.W. Langmi, G. Sean McGrady, Xiangfeng Liu, C.M. Jensen, J. Phys. Chem. C 114 (2010) 10666–10669, https://doi.org/10.1021/jp102641p.
[10] Fuqiang Zhai, Ping Li, Aizhi Sun, Shen Wu, Wan Qi, Weina Zhang, Yunlong Li, Liqun Cui, Xuanhui Qu, J. Phys. Chem. C 116 (2012) 11939–11945, https://doi.org/10.1021/jp302721w.
[11] M. Ismail, A.M. Sinin, C.K. Sheng, W.B. Wan Nik, Int. J. Electrochem. Sci. 9 (2014) 4959–4973.
[12] W.G. Brown, Org. React. 6 (1951) 469, https://doi.org/10.1002/0471264180.or006.10.
[13] https://en.wikipedia.org/wiki/Lithium_aluminium_hydride.
[14] O. Palumbo, A. Paolone, P. Rispoli, R. Cantelli, Mater. Sci. Eng. A 521–522 (2009) 134–138.
[15] A.S. Nowick, B.S. Berry, Anelastic Relaxation in Crystalline Solids, Academic Press, New York, 1972 (chapter 16).
[16] I.S. Golovin, V.V. Palacheva, D. Mari, G. Vuilleme, A.M. Balagurov, I.A. Bobrikov, J. Cifre, H.R. Sinning, J. Alloy. Comp. 790 (2019) 1149–1156, https://doi.org/10.1016/j.jallcom.2019.03.264.
[17] F.Q. Zu, Z.G. Zhu, B. Zhang, Y. Feng, J.P. Shui, J. Phys. Condens. Matter 13 (2001) 11435–11442.
[18] R. Montanari, A. Varone, Metals 5 (2015) 1061–1072, https://doi.org/10.3390/met5021061.
[19] E. Bonetti, E.G. Campari, L. Pasquini, E. Sampaolesi, J. Appl. Phys. 81 (1997) 7186, https://doi.org/10.1063/1.368639.
[20] Li Dong, T. Jaglinski, D.S. Stone, R.S. Lakes, Appl. Phys. Lett. 101 (2012) 251903, https://doi.org/10.1063/1.4772940.
[21] A.K. Malhotra, D.C. Van Aken, Acta Metall. Mater. 41 (1993) 1337.
[22] L. George, Surendra K. Saxena, Int. J. Hydrogen Energy 35 (2010) 5454–5470, https://doi.org/10.1016/j.ijhydene.2010.03.078.
[23] M.L. Hentschel, N.W. Page, J. Mater. Sci. 42 (2007) 1261–1268, https://doi.org/10.1007/s10853-006-1145-x.
[24] L.P. Argani, D. Misseroni, A. Piccolroaz, Z. Vinco, D. Capuani, D. Bigoni, J. Eur.

Ceram. Soc. 36 (2016) 2159–2167. https://doi.org/10.1016/j.jeurceramsoc.2016.02.012.

[25] E. Bonetti, E.G. Campari, L. Pasquini, L. Savini, Rev. Sci. Instrum. 72 (2001) 2148, https://doi.org/10.1063/1.1357235.

[26] S. Amadori, E.G. Campari, A.L. Fiorini, R. Montanari, L. Pasquini, L. Savini, E. Bonetti, Mater. Sci. Eng. A 442 (2006) 543–546, https://doi.org/10.1016/j.msea.2006.02.210.

[27] www.tainstruments.com/wp-content/uploads/dma.pdf.

[28] M.S. Blanter, Igor S. Golovin, H. Neuhäuser, Hans-Rainer Sinning, Internal Friction in Metallic Glasses, Springer Series in Materials Science, January, 2007, https://doi.org/10.1007/978-3-540-68758-0.

[29] https://www.azom.com/materials-video-details.aspx?VidID=1050.

[30] V.P. Balema, J.W. Wiench, K.W. Dennis, M. Pruski, V.K. Pecharsky, J. Alloy. Comp. 329 (2001) 108–114, https://doi.org/10.1016/S0925-8388(01)01570-5.

[31] R.A. Varin, L. Zbroniec, J. Alloy. Comp. 504 (2010) 89–101, https://doi.org/10.1016/j.jallcom.2010.05.059.

[32] J.R. Ares, K.-F. Aguey-Zinsou, M. Porcu, J.M. Sykes, M. Dornheim, T. Klassen, R. Bormann, Mater. Res. Bull. 43 (2008) 1263–1275, https://doi.org/10.1016/j.materresbull.2007.05.018.

[33] J. Cai, Lei Zang, L. Zhao, J. Liu, Y. Wang, Journal of Energy Chemistry 25 (2016) 868–873, https://doi.org/10.1016/j.jechem.2016.06.004.

[34] S. Sartori, K.D. Knudsen, B.C. Hauback, J. Phys. Chem. C 116 (2012) 3875–3881, https://doi.org/10.1021/jp206479m 648–653.

[35] J.W. Wiench, V.P. Balema, V.K. Pecharsky, M. Pruski, J. Solid State Chem. 177 (2004).

[36] T.S. Kê, Phys. Rev. 71 (1947) 533.

[37] H.G. Bohn, M. Prieler, C.M. Su, H. Trinkaus, W. Schilling, J. Phys. Chem. Solids 55 (1994) 1157–1164, https://doi.org/10.1016/0022-3697(94)90133-3.

[38] E.G. Campari, S. Amadori, E. Bonetti, R. Berti, R. Montanari, Metals 9 (2019) 549–557, https://doi.org/10.3390/met9050549.

[39] Magnus J. Lipp, Zs Jenei, H. Cynn, Y. Kono, C. Park, C. Kenney-Benson, W.J. Evans, Nat. Commun. 8 (2017) 1198, https://doi.org/10.1038/s41467-017-01411-9.

[40] M. A. Carpenter, Rev. Mineral. Geochem., DOI :10.2138/rmg.2000.39.02.

[41] Guo-Hua Ding, Xuan Qi, Shu-Long Liu, Ming Li, Jing Hu, J. Mater. Res. 31 (2016) 1145, https://doi.org/10.1557/jmr.2016.118.